NUMERICAL INVESTIGATION ON FLOW CONTROL BY COMPRESSIBLE TURBULENT WALL JETS (VERIFICATION OF TURBULENCE MODELS)

Kentaro Watanabe
Graduate School, Science University of Tokyo
1-3 Kagurazaka Shinjuku-ku Tokyo 162-8601, Japan
j4500650@ed.kagu.sut.ac.jp

Kazuyuki Toda
Department of Mechanical Engineering, Science University of Tokyo
1-3 Kagurazaka Shinjuku-ku Tokyo 162-8601, Japan
ktoda@rs.kagu.sut.ac.jp

Makoto Yamamoto
Department of Mechanical Engineering, Science University of Tokyo
1-3 Kagurazaka Shinjuku-ku Tokyo 162-8601, Japan
yamamoto@rs.kagu.sut.ac.jp

ABSTRACT
If separation occurs in a flow field, it causes a large pressure loss and thus aerodynamic performance is largely reduced. A wall jet, i.e. tangential blowing, is one of the control techniques for such a flow field. However, the verification of turbulence models for a wall jet in compressible flow is insufficient. In the present study, we examine the predictive performance for five typical turbulence models (Spalart-Allmaras 1 eq. model, Lam-Bremhorst, Myong-Kasagi and Shimada-Nagano k–ε 2 eq. models and Craft-Launder-Suga k–ε–A_2 3 eq. model). In the results, the k–ε models show a relatively good predictive performance and little difference of distributions among the models. On the other hand, Spalart-Allmaras and Craft-Launder-Suga models indicate the inclination to overestimate the size of separation region.

INTRODUCTION
In order to realize a high-speed transport, recently super/hypersonic airplanes have been developed actively. However, there remain many technical problems to be overcome. To design and develop a shorter air intake is one of the key subjects. Since the cruising Mach number restricts the length of the supersonic part of the intake, the possibility of improvement is laid on the subsonic part (i.e. diffuser). However, if we adopt a large diffuser angle to shorten the subsonic part, flow separation occurs in the diffuser passage, and thus the intake performance is considerably reduced. Accordingly, the separation control is an essential part of the subjects to maintain and improve the intake performance.

A wall jet, i.e. tangential blowing, is the representative technique to remove or suppress such separation. We can control the separation and decrease the energy loss by giving kinetic energy to the lower momentum fluid in the boundary layer near a wall. In the previous study, we investigated the effect of a wall jet on the diffuser performance numerically, and indicated the possibility of foreshortening the diffuser length (Yoshikawa et al., 1999). On the other hand, all results obtained from the numerical simulation showed the inclination to overestimate the suppression effect for the separation bubble. Then, we suspected that the trend was attributed to the predictive performance of a turbulence model, but could not conclude because the predictive performance of the turbulence models, especially for the compressible turbulent wall jet, have never been clarified. Under these backgrounds, the purpose of this study is put on the clarifying the predictive performance of the turbulence models for the compressible turbulent wall jet. Five representative turbulence models are focused on and three flow fields with a wall jet are considered.

Type	Proposer	
1 eq. Model	Spalart-Allmaras (1992)	SA
2 eq. Model	Lam-Bremhorst (1981)	LB
	Myong-Kasagi (1988)	MK
	Shimada-Nagano (1996)	SN
3 eq. Model	Craft-Launder-Suga (1997)	CLS

Table 1 : Turbulence models

TURBULENCE MODEL
In this study, we verify the predictive performance of turbulence models for the compressible turbulent wall jets and back-step flows. 5 representative turbulence models are focused on, and they are summarized in Table 1. Although a lot of

modifications have been proposed to reflect the compressible effects into the model, we do not introduce any such extensions due to the lack of generality.

NUMERICAL PROCEDURES

Considering the computational stability and accuracy, following numerical procedures were introduced in our computations. The mass-averaged Navier-Stokes equations were solved explicitly to avoid the complexity in the numerical code. 4^{th}-order Runge-Kutta method with local time step technique was adopted into time integration, taking into account of the steady state flow calculation. 2^{nd}-order upwind TVD scheme by Harten-Yee (1987) was employed for convection terms and 2^{nd}-order central difference scheme for another terms. It was assumed that converged solutions were attained when the non-dimensional residuals for all equations become simultaneously less than 10^{-6}.

COMPUTATIONAL CONDITIONS

The flow fields considered for model validation were 3 wall jets and 2 back-step flows. Computational conditions for each flow are explained below.

Case1: Blowing into Stationary Fluid

First, we verify the predictive performance of the turbulence models for a flow field with an incompressible turbulent wall jet to clarify the Mach number dependency. Furthermore, we consider that this flow field is important to verify the predictive performance of turbulence models such as SA model that was developed for the compressible turbulent flows. Fig. 1(a) shows the schematic of the flow field in this case. The geometry of the computational domain is 442mm in x direction and 88mm in y direction. The blowing slit with H=10mm height is embedded on the lower portion of the left-side wall (x=0mm). Reynolds number based on the slit height and the inlet mean velocity is $Re = 1.0 \times 10^4$. These computational conditions follow the experiment by Karlsson et al. (1996). Computational grid used in this case has 101 points in x direction and 103 points in y direction. The grid-points beside the each solid surface are arranged to satisfy y^+ = 0.7 to 2.5.

Case2: Blowing into 2D Channel Flow

Case2 is the 2D channel flow with a wall jet of sonic speed. In this case, we investigate the basic characteristic of the models for the compressible turbulent wall jet. The flow field is schematically depicted in Fig. 1(b). The computational domain with 80×11mm is considered, and the blowing slit with H=1mm height is located on the lower wall 20mm downstream from the inlet boundary. The mainstream and blowing conditions are summarized in Table 2. Reynolds number based on the step height and the mainstream maximum velocity is $Re = 2.9 \times 10^4$. Computational grid used in this case has 101 points in each direction, and is disposed for y^+ to be 0.8 to 1.5 at the first grid points from the wall.

		Casae2	Case3
Main-stream	Mach Number	0.8	3.4
	Total Pressure [kPa]	250	816
	Total Temperature [K]	285	297
	Boundary Layer Thickness [mm]	2.1	0.41
Blowing	Mach Number	1.0	3.5
	Total Pressure [kPa]	250	655
	Total Temperature [K]	285	297
	Boundary Layer Thickness [mm]	33.0	0.0

Table 2 : Mainstream and Blowing Conditions

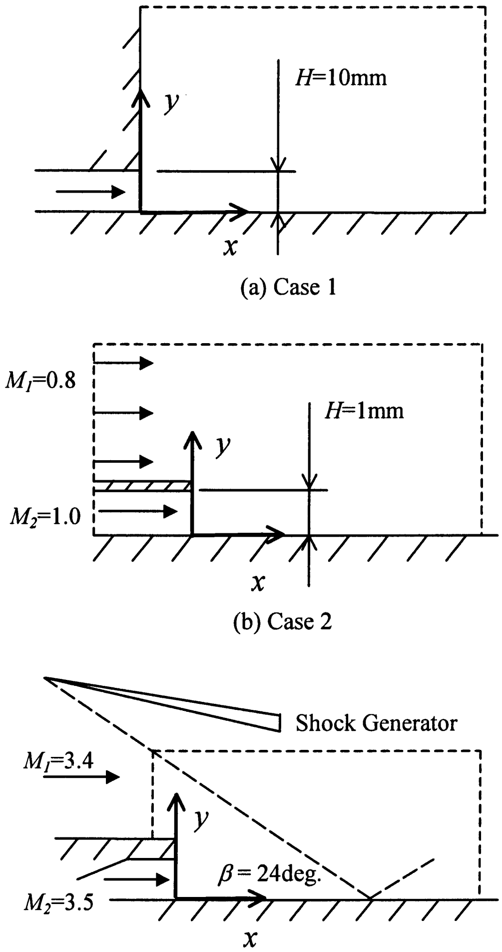

(a) Case 1

(b) Case 2

(c) Case 3

Figure 1 : Schematic of Flow Fields

Case3: Blowing into Shock Wave/Turbulent Boundary Layer Interaction Region

The third case is the more practical one. Controlling the shock wave/turbulent boundary layer interaction, which frequently appears in the supersonic turbulent flow fields, is very important for the purpose of engineering. Numerical simulation is very helpful for understanding the details of the flow structure. In this case, the supersonic turbulent flow field with secondary flow blowing tangentially into the shock/turbulent boundary layer interaction region is computed, as shown in Fig. 1(c). The geometry of the computational domain is 325mm in x direction and 36mm in y direction. The blowing step with H=12.7mm height is located on the lower wall 60mm downstream from the inlet boundary. The mainstream and blowing conditions are summarized in Table 2. Reynolds number based on the step height and the mainstream maximum velocity is $Re = 2.3 \times 10^5$. The secondary flow (tangential blowing) is assumed not to have any boundary layer and hence the velocity profile at the blowing boundary is assigned uniformly. Incident angle of the shock wave is 24 degrees and it reflects with the lower wall at x_{Imp}=181mm. These computational conditions follow the experiment by Donovan et al. (1996). The computational grid composed of 101×111 points are provided in this case, and the points are clustered around the shock reflecting point in x direction and solid wall in y direction. With this arrangement, the value of y^+ always becomes 0.1 to 0.4 at the first grid points from the wall.

RESULTS AND DISCUSSIONS

Case1: Blowing into Stationary Fluid

Fig. 2 compares the mean velocity profiles of x direction with experimental data on the three different downstream cross sections. The result with each k–ε model (LB, MK and SN) shows good agreement with the experimental data. On the other hand, SA model predicts the faster velocity recovery, and hence it can be suggested that SA model

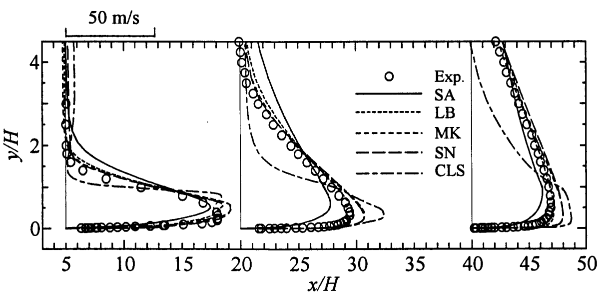

Figure 2 : Profiles of Velocity Component u (Case1)

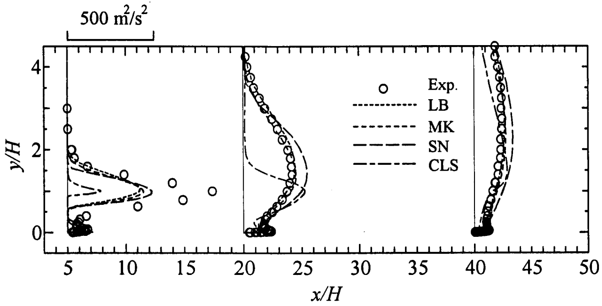

Figure 3 : Profiles of Turbulent Energy k (Case1)

Turbulence Model	Lr / H
Spalart-Allmaras model	7.52
Lam-Bremhorst model	5.37
Myong-Kasagi model	5.93
Shimada-Nagano model	6.42
Craft-Launder-Suga model	8.07

Table 3 : Reattachment Length (Case2)

overestimates the turbulent viscosity in a low Mach number flow. In contrast, CLS model reproduces excessively large maximum velocity in every cross section. Therefore, CLS model is thought to have the tendency to underestimate the turbulent diffusivity.

In Fig. 3, the profiles of turbulent kinetic energy are compared with experimental data in the same cross sections as those in Fig. 2. While each k–ε model again shows good agreement with the experimental data, CLS model reproduces the relatively smaller turbulent kinetic energy in all sections. The inclination for CLS model to underestimate the turbulent diffusivity, supposed from the previous velocity profiles, may be attribute to this lower kinetic energy level.

Case2: Blowing into 2D Channel Flow

Fig. 4(a) compares the velocity distributions in the case without blowing (i.e. back-step flow), and Fig. 4(b) those with blowing. From these figures, each k–ε model reproduces the similar result, and hence it can be suggested that the difference of model performances is small. Fig. 4(b) indicates that SA

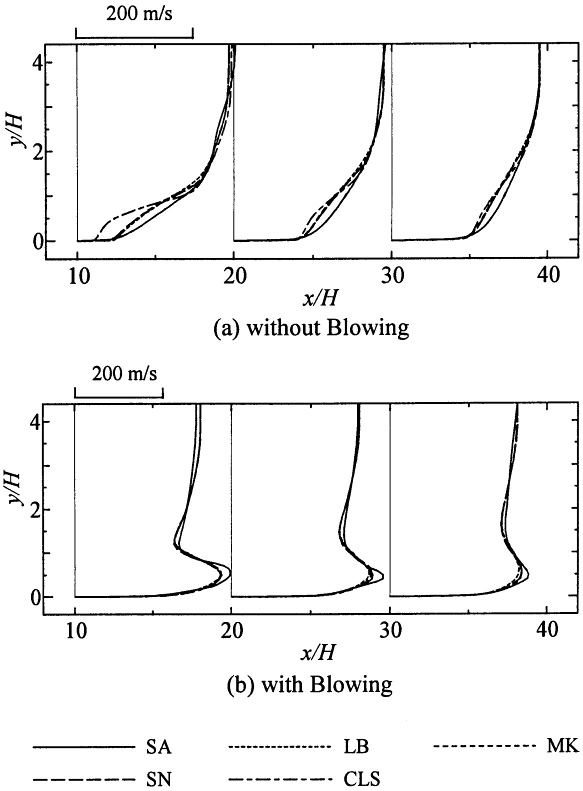

Figure 4 : Profiles of Velocity Component u (Case2)

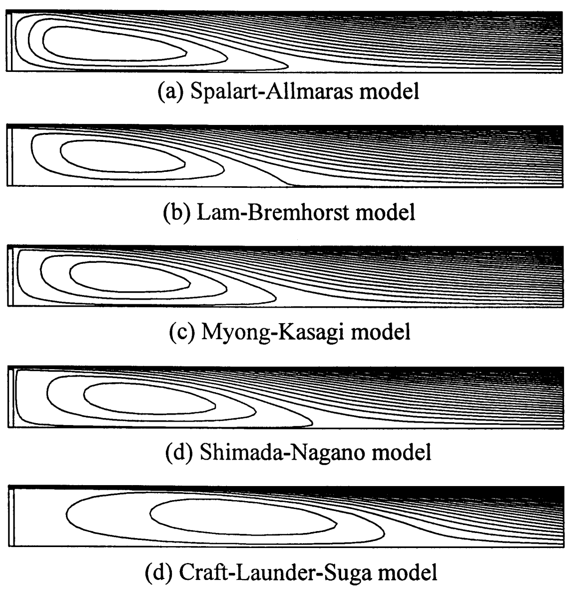

(a) Spalart-Allmaras model

(b) Lam-Bremhorst model

(c) Myong-Kasagi model

(d) Shimada-Nagano model

(d) Craft-Launder-Suga model

Figure 5 : Stream Lines (Case2)

model reproduces the smaller turbulent viscosity than that of k-ε models in the case with blowing because of the slower velocity recovery. In this case, CLS model predicts approximately the same distributions as those with k–ε models.

For the case without blowing, the streamlines are presented in Fig. 5, and reattachment length behind the step, Lr, are listed in Table 3, where Lr is normalized by the step height H. CLS model predicts apparently larger separation bubble, and this trend is also appeared in the reattachment length. Thus, the trend of CLS model to underestimate the turbulent viscosity for the separated flow is pointed out again.

Case3: Blowing into Shock Wave/Turbulent Boundary Layer Interaction Region

Fig. 6 compares the velocity profiles of x direction in the different cross sections for the case with shock/turbulent boundary layer interaction. Fig. 6(a) shows the case without blowing (just like a back-step flow) and Fig. 6(b) with blowing. In both cases, each k–ε model reproduces approximately the same result. This tendency is consistent with that shown in Case2. SA and CLS models predict an excessively large separation bubble in the case without blowing. This separation extends from the step to the shock reflecting point, and the scale is much larger than that obtained by k–ε models. On the other hand, in the case with blowing, both models show only a little higher diffusivity, and almost the similar distributions to that of k–ε models, as shown in Fig. 6(b). Accordingly, these results suggest that the difference of the predictive performance among the models would hardly appear in the case with blowing, where the boundary layer separation does not exist.

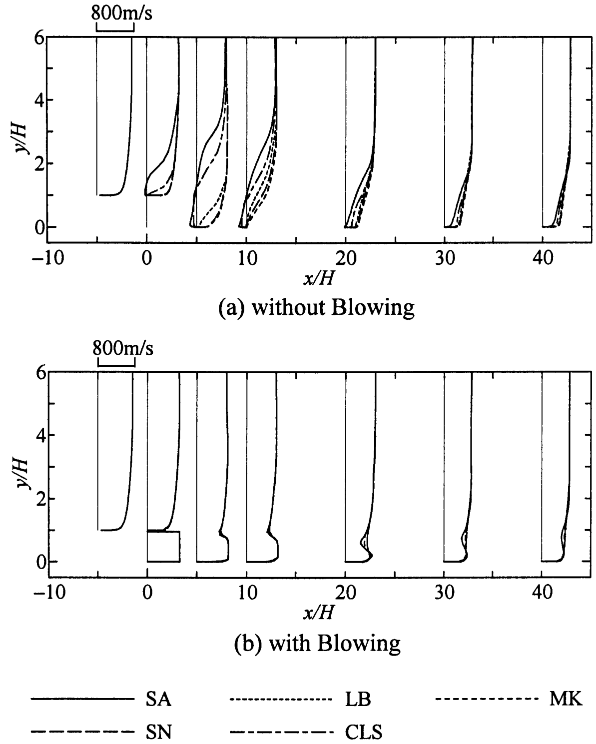

Figure 6 : Profiles of Velocity Component u (Case3)

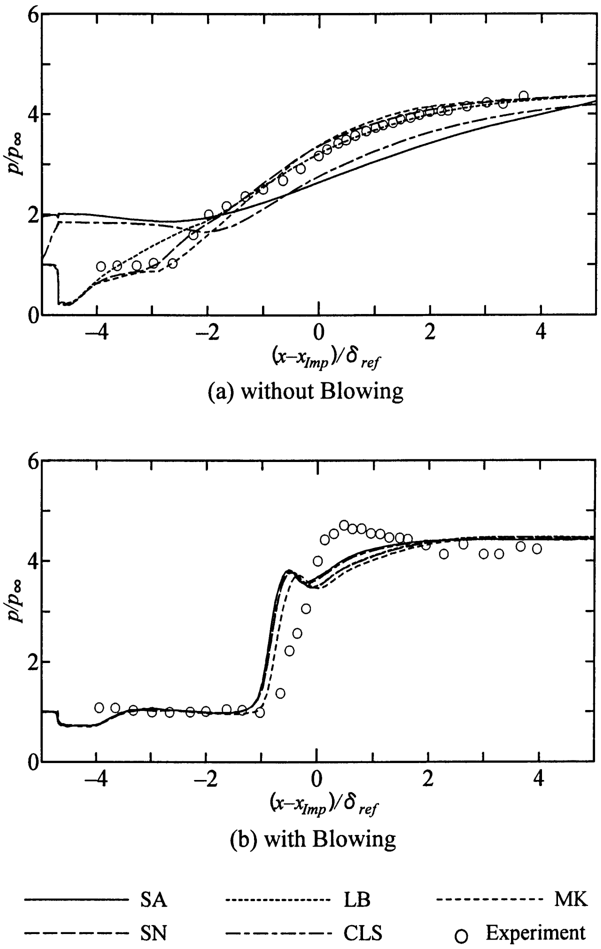

Figure 7 : Profiles of Wall Static Pressure (Case3)

The profiles of wall static pressure are compared with experimental data in Fig. 7. The vertical and horizontal axis are normalized by static pressure p_∞ and boundary layer thickness δ_{ref} respectively, which are obtained upstream of the step. As shown in Fig. 7(b), all models predict approximately the same profiles in the case with blowing. On the other hand, there is a remarkable difference among the results in the case with blowing. Each k–ε model predicts approximately the same result that is in good agreement with experimental data, while the inclination of SA and CLS models to overestimate the separation region appears again. Although the inclination of SA model to overestimate the separation region is exceedingly strong compared with that shown in Case2, SA model predicts approximately the same result as those with k–ε models in the case with blowing. Therefore, it can be considered that SA model can supply the reasonable result for an attached boundary layer or a flow separation not affected by shock wave, but there is a problem in predicting the separation induced by shock wave/turbulent boundary layer interaction.

Verification of the Predictive Performance of CLS Model with Incompressible Code

In the current study, we have investigated the predictive performance of turbulence models for 3 wall jets and 2 back-step flows. In the context, CLS model showed the consistent characteristic to underestimate the turbulent viscosity in all cases. On the other hand, it is reported that CLS model can reproduce the reasonable result for 2D back-step flow using a computational code for incompressible flow (Suga et al., 2000). Then, we decided to calculate a back-step flow under the same condition as the report, using an incompressible code with MAC method, for the purpose of clarifying the dependence of numerical procedures for CLS model. The flow field focused on in this case has Reynolds number Re=5000 based on the step height H and the maximum inflow velocity, and the expansion rate of the flow passage is 1.5. Computational grid used in this case has 80×90 points in each direction. The grid-points near the wall are located so that $y^+= 0.01$ to 0.2. Governing equations are discretized with finite difference method. 3rd-order upwind difference scheme by Kawamura and Kuwahara was employed for the convection terms and 2nd-order central difference scheme for another terms.

In this computation, strong unsteadiness was appeared, and this is thought to be responsible for underestimation of the turbulent viscosity. Contrarily, such unsteadiness was not seen in Case1, 2 and 3. Some of the reasons for this difference can be point out as follows. First, in the former cases (Case1, 2 and 3), the local time step technique was applied to the time integration, according to the assumption of steady state solution. Second, TVD scheme used in

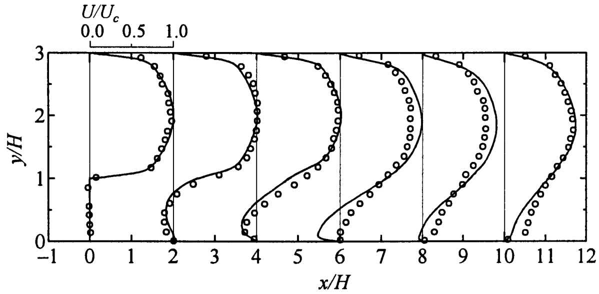

Figure 8 : Profiles of Velocity Component u

the compressible code (former 3 cases) would contribute the solution to be a steady state due to the artificial diffusion.

The velocity profiles, compared with the experimental data in Fig. 8, are obtained by temporally averaging the transient distributions. We can confirm that CLS model underestimates the turbulent diffusivity again. Also in this case, we obtained a consistent opinion that CLS model underestimates turbulent viscosity even with an incompressible code, as well as Case1, 2 and 3. Accordingly, our result is in conflict with the report mentioned previously. The considerable reason for this difference will be thought to attribute to some special techniques introduced in the report related to the implicit procedure. In our preliminary calculation, CLS model provided the reasonable profiles for an attached boundary layer. Taking account of above results, it is suggested that CLS model tends to assess the smaller turbulence level in the recirculation zone, depending on the numerical procedures.

CONCLUSIONS

In this study, we calculated 3 wall jets and 2 back-step flows with 5 different turbulence models. Comparing the results among the models, and with experimental data, we obtained following conclusions.

1. There is little difference of predictability among k–ε models (LB, MK and SN), regardless of flow compressibility. The results are always in reasonable agreement with the experimental data.
2. SA model overestimates a size of separation bubble induced by shock wave/turbulent boundary layer interaction. Thus, it is not suitable for predicting such a flow field.
3. CLS model tends to assess the smaller turbulence level in the recirculation zone, provably depending on the numerical procedures.

ACKNOWLEDGEMENT

In this study, we got a lot of advices from Dr. Kazuhiko Suga (Toyota Central Laboratory) relating to a coding of k–ε–A_2 model and its predictive performance. We would like to express our special gratitude. This research has partly been supported through the Grant-in-Aid for Scientific Research (No. 1265018) by the Ministry of Education, Science and Culture, and the foundation (No. REDA S00-7) by the Fundamental Research Developing Association for Ship Building and Offshore.

References

Craft, T., J., Launder, B., E., and Suga, K., 1997, "Prediction of turbulent transitional phenomena with a nonlinear eddy-viscosity model", *Int. J. Heat and Fluid Flow*, Vol.18, No.1, pp.15-28

Donovan, J., F., 1996, "Control of Shock Wave/ Turbulent Boundary Layer Interactions Using Tangential Injection, *AIAA Paper*, 96-043

Karlsson, R., I., Eriksson, J., and Persson, J., 1996, "LDV Measurements in a Plane Wall Jet in a Large Enclosure",*6th Int. Symposium on Applications of Laser Techniques to Fluid Mechanics*, pp.1.1.5-1.1.6

Lam, C. K. G., and Bremhorst, K. A., 1981, "A Modified Form of the k–ε Model for Predicting Wall Turbulence", *Trans. ASME, J. Fluid Eng.*, 103, pp.456-460

Myong, K., and Kasagi, N., 1988, "New Proposal for k–ε Turbulence Model and Its Evaluation (2nd Report, Evaluation of the Model)", *Trans. of JSME, Ser. B*, 54-508, pp.3512-3520

Shimada, M., and Nagano, Y., 1996, "Advanced Two-Equation Turbulence Model for Complex Flows in Engineering", *Engineering Turbulence Modeling and Experiments 3*, pp.111-120

Spalart, P. R., and Allmaras, S. R., 1992, "A One-Equation Turbulence Model for Aerodynamic Flow", *AIAA Paper*, pp.92-0439

Suga, K., Nagaoka, M., Horinouchi, N., Abe, K., and Kondo, Y., 2000, "Application of a Three Equation Cubic Eddy Viscosity Model to 3-D Turbulent Flows by the Unstructured Grid Method", *Turbulence, Heat and Mass Transfer 3*, pp.373-380

Yee, H., C., and Harten, A., 1987, "Implicit TVD Schemes for Hyperbolic Conservation Laws in Curvilinear Coordinates", *AIAA J.*, 25, pp.266-274

Yoshikawa, N., Yamamoto, M., and Honami, S., 1999, "Numerical Simulation of Subsonic Diffuser for Supersonic Air-Intake (Effect of Blowing on Diffuser Performance)", *Trans. of JSME, Ser. B*, 65-631, pp. 876-881